

On the Localization of Sensors using a Drone with UWB Antennas

Francesco Betti Sorbelli
Dept. of Computer Science and Math.
University of Florence, Italy
francesco.bettisorbelli@unifi.it

Cristina M. Pinotti
Dept. of Computer Science and Math.
University of Perugia, Italy
cristina.pinotti@unipg.it

Abstract

In the last years, mega-wildfires have become routine news. For the firefighters, it is crucial to rely on systems able to prevent and detect those disastrous events. Wireless Sensor Networks (WSNs) become an important issue such as environmental and forest monitoring. An important requirement for the WSNs is the ability to precisely localize their sensors for augmenting the collected data with their position. In this paper, we survey three previous presented algorithms, called SHORT, DIR, and OMNI, for localizing terrestrial sensors using a drone. We compare their performance under a variety of different conditions: we evaluate the path length, we compare the localization performance in terms of precision and error, and we analyze the impact of using multilateration instead of trilateration during each localization. Our study supports the importance of the geometry in selecting the waypoints from which a sensor is measured. The common belief that multilateration leads to a more precise localization is not completely correct. Indeed, we have shown by simulations that, when the waypoints follow a well pondered geometry, multilateration is not useful. Whereas, the multilateration can improve the precision for algorithms that select the waypoints according to a best-effort policy.

1 Introduction

It is widely known that, during the dry season, the risk to have a forest fire is very high. Every year, such situations create huge damages in terms of money and even in terms of human lives. Nowadays, we are used to watch on television firefighters that try to extinguish fires where the majority of which are caused from humans fraudulently. Therefore, it is appropriate to build robust solutions for fire fighting in order to prevent and detect such emergencies. As an example, the Mediterranean basin, which is a very large area, is continuously affected by fires in the summer. Hence, it is required to cover and precisely monitor these potential hazardous areas by sensors.

In such scenario, a Wireless Sensor Network (WSN) can be built inside a forest for monitoring tasks. Deploying sensors close to dangerous places is essential in order to detect potential clues, for example, unexpected temperature increases in a very dry zone. Once the detected data from the terrestrial sensors are delivered to the master

Copyright © by the paper's authors. Copying permitted for private and academic purposes.

In: G. Di Stefano, A. Navarra Editors: Proceedings of the RSFF'18 Workshop, L'Aquila, Italy, 19-20-July-2018, published at <http://ceur-ws.org>

gateway node, proper and adequate solutions are taken. To build the WSN, sensors can be randomly deployed in the target area and a mobile vehicle can be used to be the contact point between the WSN and the external world. Therefore, the random deployment results in sensors initially unaware of their location. Localization is one the most important task in a WSN, since it provides fundamental support for many location-aware protocols and applications. Due to limitations in form factor, cost per unit, and energy budget, individual sensors are not expected to be GPS-enabled. Many existing localization algorithms in the literature require a large number of fixed anchor points, i.e., sensors whose positions are known a-priori [1]. The number of the anchor points and the cost of their deployment grow with the size of the deployment area. Moreover, the anchor points must be deployed in advance, making the use of anchor sensors unsuitable for emergency situations.

In order to decrease the setup costs of WSNs, we propose to replace fixed anchor sensors with a single mobile anchor sensor, such as an Unmanned Aerial Vehicle (UAV) [2, 3]. Recently, UAVs, also known as drones, have received increasing attention from research and industry community [4, 5]. Depending on the adopted technique to estimate the sensors' positions, localization algorithms can be categorized in *range-free* or *range-based*. In the former case, the position estimation is performed without using any type of ranging measurements. In the latter, the estimations are instead inferred by exploiting several properties of the communication signals, such as the Received Signal Strength Indicator (RSSI) or the Time of Arrival (ToA).

In this paper, we survey three previous presented algorithms: SHORT [6], DIR [3], and OMNI [2]. All the three algorithms are range-based and use a drone as a mobile anchor, which replaces the fixed anchors. The original contribution of this work is a comparative study via simulation of the properties of these three localization algorithms. Moreover, we extend the three algorithms by using, to localize the sensors, multilateration instead of trilateration. Our somehow counterintuitive finding is that multilateration does not always improve the precision of the localization, especially when the trilateration has selected measurements that reflects a peculiar geometry.

The three algorithms make different assumptions of the available hardware at the drone for communicating with the terrestrial sensors. DIR assumes that the drone is equipped with directional antennas, which can adjust their beamwidth according to the required precision. SHORT and OMNI assume only a regular omnidirectional antenna. All the solutions adopt the Impulse-Radio Ultra-Wide-Band (IR-UWB) technology for the antennas. DIR and OMNI are based on a static path for the drone over the deployment area, and guarantee the localization precision required by the final user, while SHORT produces a very short static path, but it cannot guarantee any a-priori localization precision. Again, DIR and OMNI prefer precision to path length, whereas SHORT sacrifices precision for being able to accomplish an entire mission without recharging the battery.

It is very important to stress that all the three algorithms locate all the nodes independently of their number and their actual position. While traversing the path, the drone calculates the distances with the sensors at special positions, called waypoints: each waypoint acts as a fixed anchor node. Once a sensor has received three measurements, it can calculate its position by applying the trilateration procedure. Moreover, in this paper, to localize themselves, the sensor can either perform a multilateration using six different measurements or the usual trilateration procedure.

The main contribution of this work is to present an extensive comparison of the three algorithms that studies, in particular, whether using a greater number of measurements for each sensor is possible to increase the localization precision. Our findings contradict the common belief that multilateration always help.

The rest of paper is organized as follows. Sec. 2 revises the current literature on localization algorithms using drones. Specifically, in Sec. 2.1, we survey SHORT, in Sec. 2.2, we survey DIR, while in Sec. 2.3, we survey OMNI. The experimental results are discussed in Sec. 3, while Sec. 4 concludes the paper.

2 Recent Localization Algorithms

We consider a network of n sensors deployed in a rectangular area Q of size $Q_x \times Q_y$. From now on, sensor P is short form for the sensor that resides at a point P in Q . Since, in principle any point P in Q is candidate to contain a sensor, with a little abuse of notation, we denote P indistinctly as the point P or the sensor P . Moreover, we use the notation $\overline{PP'}$ to denote the ground distance between two waypoints/sensors P and P' .

Our mobile anchor is a drone. It flies at a fixed altitude h [7]. We assume that the drone measures its altitude with negligible error, for example, by using the Differential GPS technique [8]. To range the sensors on the ground and to achieve higher precision, we adopt the two-way ranging application of the IR-UWB technology, which guarantees a very high measurement precision of the order of 10 cm [9], but other technologies could be used as well. For example, WiFi guarantees an instrumental precision of 7-10 m, and Bluetooth of 15 m [10].

Static Path

In recent years, autonomous vehicles have been used for patrolling areas. Since in this work we assume that the autonomous vehicle is a drone, the trajectory will be traversed at a certain altitude h and the projection on the ground of the trajectory will be denoted as 2D movement trajectory.

Assuming that the path is used for localizing objects, the drone will take the measurements at predefined points along its trajectory. The projection on the ground of a measurement point will be called *waypoint*.

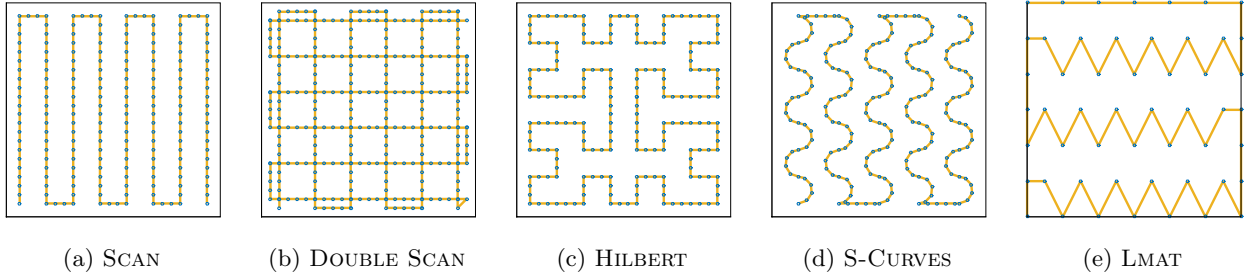


Figure 1: Different movement trajectories.

In [11], three different 2D movement trajectories have been studied, i.e., SCAN, DOUBLE SCAN and HILBERT. The simplest algorithm is SCAN (see Fig. 1(a)), in which the drone follows a path formed by vertical straight lines interconnected by horizontal lines. Essentially, the drone sweeps the area along the y -axis and the waypoints are regularly distributed along the path. The main drawback is that SCAN provides a large amount of collinear anchor points. In order to resolve the collinearity problem, DOUBLE SCAN has been proposed (see Fig. 1(b)), in which the mobile anchor node sweeps the sensing area along both the x -axis and the y -axis. However, in this way the path length is doubled compared with SCAN. A level- n HILBERT (see Fig. 1(c) with $n = 3$) curve divides the area into 4^n square cells and connects the centers of those cells using 4^n line segments, each of length equal to the length of the side of a square cell. HILBERT provides more non-collinear anchor points but the path length can be very long if the value of the parameter n increases. Note that, all the above three schemes are based on straight lines. In order to heavily reduce the collinearity during localization, the S-CURVES (see Fig. 1(d)) static path was introduced in [12]. S-CURVES is similar to SCAN except that it uses curves rather than straight lines. Even though the collinearity problem is almost resolved, the main problem is that it does not cover properly the four corners of the square sensing area. The authors in [13] developed LMAT (see Fig. 1(e)): the main idea is to plan a series of mobile anchor points in such a way as to form regular equilateral triangles, avoiding collinearity problems. Each node inside a triangle is localized by a trilateration procedure using the three vertices.

It is worthy to note that DIR and OMNI adopt a SCAN 2D trajectory. SHORT, instead, starts with a trajectory similar to LMAT, which is then modified by solving an instance of the Traveling Salesman Problem (TSP).

Measurement Definitions

In all the three algorithms compared in this work, i.e., SHORT, DIR, and OMNI, during the mission the drone takes measurements at pre-established points of the path called waypoints.

We assume that the drone, using the IR-UWB antenna, measures its distance from the sensors by the round-trip time of messages exchanged with them. To take a measurement, the drone acts as follows. At each waypoint w_i , the drone sends a beacon signal with a unique identifier which depends on the coordinates (x_{w_i}, y_{w_i}) of the waypoint and the current timestamp. Each sensor on the ground that can hear a beacon replies to the drone with an ack message that contains its ID, the current timestamp, and the identifier of the beacon received. The drone computes the distance between itself and the sensor using the round-trip time of the beacon message and then sends a message with the computed distance to the sensor. Once a sensor has collected three measurements, it can locally apply the trilateration algorithm (Eq. (1)) to discover its position P . Hence, given three ground measures, the estimated position of P is the point (x_P, y_P) that minimizes the sum of the least squares, that is:

$$\min \delta_1^2 + \delta_2^2 + \delta_3^2 \quad \text{s.t.} \quad \sqrt{(x_{w_i} - x_P)^2 + (y_{w_i} - y_P)^2} + \delta_i = \overline{w_i P} \quad \text{for } i = 1, 2, 3 \quad (1)$$

The multilateration (in our case, a six-lateration) procedure can be considered as the generalization of trilateration, as reported in Eq. (2), when six measurements are considered:

$$\min \sum_i \delta_i^2 \quad \text{s.t.} \quad \sqrt{(x_{w_i} - x_P)^2 + (y_{w_i} - y_P)^2} + \delta_i = \overline{w_i P} \quad \text{for } i = 1, \dots, 6 \quad (2)$$

Distance Definitions

The drone and the sensor have communication ranges, r_{drone} and r_{sensor} , respectively. Since a message can be exchanged between the drone and the sensor only if they can hear each other, throughout this paper, the communication range will be $r = \min\{r_{\text{drone}}, r_{\text{sensor}}\}$.

The drone measures the (3D) *slant distance* s , which is defined as the line-of-sight between itself and the measured sensor. Clearly, $s \leq r$. By simple geometric argument, since we assume negligible error in altitude, it is easy to see that any *ground* measured distance d satisfies:

$$d = \sqrt{s^2 - h^2} \leq \sqrt{r^2 - h^2} = d_{\text{max}} \quad (3)$$

In other words, slant distances when projected on the ground cannot be larger than d_{max} . This d_{max} constraint holds for all the three surveyed algorithms.

Ground and Trilateration Precision

Slant distances are affected by errors that depend on the adopted technology [10], i.e., IR-UWB in our case. The *slant precision* ϵ_s denotes the maximum error in the measurements. The trilateration algorithm works on the ground distances, thus the *ground error* $e_d(P)$ for a point P on the ground is [10]:

$$e_d(P) = \epsilon_s \cdot \frac{1}{\cos(\alpha)} = \epsilon_s \cdot \sqrt{1 + \frac{h^2}{d^2}} \quad (4)$$

where α is the angle of incidence of the slant distance to the ground, d is the distance on the ground between the drone and the sensor, h is the altitude, and ϵ_s the actual measured slant distance error (see Fig. 2).

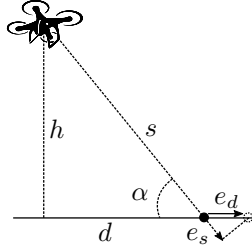


Figure 2: Relationship between slant error and ground error

From Eq. (4), the ground error increases when the ground distance decreases. Since the slant error is maximum when the distance on the ground is minimum, fixed d_{min} as the minimum allowed ground distance, the maximum possible ground error is [10]:

$$\epsilon_d = \max_{P \in Q} e_d(P) = \epsilon_s \cdot \sqrt{1 + \frac{h^2}{d_{\text{min}}^2}} \quad (5)$$

However, only DIR and OMNI are interested in bounding the localization error so, the d_{min} constraint is required only for them.

Moreover, to minimize the *localization error* $e_L(P)$ due to the trilateration, the three waypoints from which a sensor is measured cannot be collinear neither among them nor collinear with the sensor [10]. In fact, if the waypoints are collinear among them, the trilateration algorithm cannot distinguish between the real position P of the sensor and the mirror image P' of P . With regard to the collinearity with the sensor, as proved in [10], the *localization precision* ϵ_L is expressed as:

$$\epsilon_L = \max_{P \in Q} e_L(P) = \frac{\epsilon_d}{\sin\left(\frac{\beta_{\text{min}}}{2}\right)} \quad (6)$$

where β_{min} is the minimum angle obtained during the localization. The best case occurs when $\beta_{\text{min}} = \pi/3$ [10]. If the waypoints are collinear with the sensor, β_{min} tends to 0 and the localization error becomes very large and thus the estimated position very imprecise.

For the same reason mentioned above, the β_{\min} constraint is satisfied only for DIR and OMNI since they need to bound the localization error. β_{\min} is not actually satisfied in SHORT because the built geometry by triangles does not allow to bound the minimum angle β_{\min} . For example, if a generic point P resides in the midpoint of a triangle's side, d_{\min} is respected but $\beta_{\min} = 0$.

To summarize, the aim of the precise DIR and OMNI algorithms is to obtain an ϵ_L -precise localization for each point, where the maximum localization error ϵ_L is determined as a function of d_{\min} and β_{\min} . In conclusion, the sensor P in Q is ϵ_L -precisely localized, where ϵ_L is given by Eq. (6), if the drone chooses three ranging waypoints $w_1(P)$, $w_2(P)$ and $w_3(P)$ for P such that they satisfy the following constraints:

1. d_{\max} : which controls the reachability for each point P in Q : $\overline{w_i(P)P} \leq d_{\max}$ for $i = 1, 2, 3$;
2. d_{\min} : which controls the ground precision ϵ_d for P in Q : $\overline{w_i(P)P} \geq d_{\min}$ for $i = 1, 2, 3$;
3. β_{\min} : which controls the collinearity of the drone with P : $\beta(P) \geq \beta_{\min}$;
4. *non-linearity*: which controls the collinearity among waypoints: $w_1(P)$, $w_2(P)$, and $w_3(P)$ cannot belong to the same straight line.

As regard to SHORT, it only respects the reachability and collinearity constraints.

We finally resume the constraints for each algorithm in Tab. 1.

Table 1: Summary of the measurement and trilateration constraints

| | SHORT | DIR | OMNI |
|----------------------|-------|-----|------|
| d_{\max} | yes | yes | yes |
| d_{\min} | no | yes | yes |
| β_{\min} | no | yes | yes |
| <i>non-linearity</i> | yes | yes | yes |

2.1 The SHORT algorithm

SHORT assumes the drone to be equipped with a regular omnidirectional antenna. The aim of this algorithm is to find a static path as short as possible for localizing all the sensors, but any a-priori bound on the localization error is accepted. SHORT operates in two phases: *waypoint grid construction* and *waypoint ordering*.

As depicted in Fig. 3, in the first phase, SHORT builds a set of waypoints forming a grid of isosceles triangles (dashed lines) which covers the whole deployment area Q .

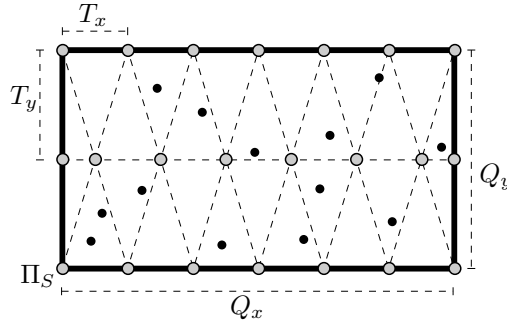


Figure 3: The waypoint grid construction phase in SHORT

The waypoints reside at the vertices of each triangle (gray dots). The triangles have the same base T_x and the same height T_y . Isosceles triangles are more flexible than equilateral ones, because they can be resized along both dimensions. This allows us to cover the whole deployment area as tightly as possible, without wasting path length for covering external areas uselessly. The base and the height of the triangles must be as long as possible, without violating the maximal triangle side d_{\max} . Given a base T_x , the longest feasible height is $T_{y_{\max}} = \sqrt{d_{\max}^2 - (T_x/2)^2}$. SHORT computes the base and the height of the triangles as follows:

$$T_x = Q_x / \left\lceil \frac{Q_x}{d_{\max}} \right\rceil \quad T_y = Q_y / \left\lceil \frac{Q_y}{T_{y_{\max}}} \right\rceil$$

Finally, in the *waypoint ordering* phase, SHORT executes the TSP solver to connect all the waypoints in order to drastically reduce the path length. The TSP solver takes in input all the waypoints' locations and gives in

output the static path Π_S . An example of Π_S is depicted as a dashed line in Fig. 4, where the gray dots represent the waypoints, while the black dots are the sensors inside Q .

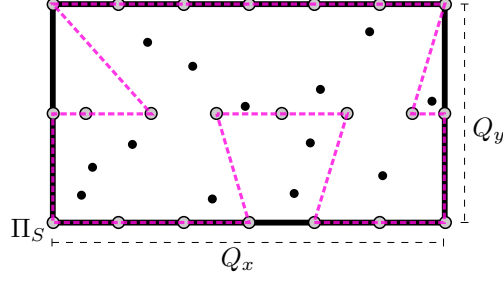


Figure 4: The static path Π_S of SHORT after the TSP

During the flight, for each waypoint, the drone sends a beacon with its position. According to the tessellation (see Fig. 3), each point P resides inside a logical isosceles triangle and it chooses the three associated vertices as its waypoints. After that, a trilateration or a multilateration procedure is performed to localize each sensor.

2.2 The DIR algorithm

DIR assumes the drone to be equipped with directional antennas. The drone is equipped with an array of six directional antennas. Each antenna is assumed to transmit the beacon in a circular sector, centered at the antenna position, of radius r , beamwidth 2θ , where $\theta = \arctan \frac{I_w/2}{d_{\min}}$, and orientation ψ .

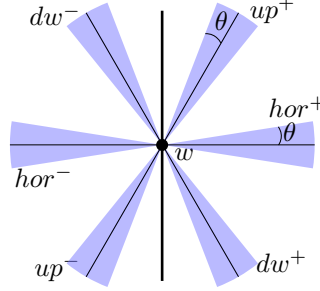


Figure 5: Possible antenna orientations

In our solution the directional antennas cover six different sectors, as illustrated in Fig. 5. The drone can send at the same time the beacons in all six orientations using an array of directional antennas [14]. Note that the sensors on the ground are equipped with omnidirectional antennas. We express each orientation ψ as a pair: *type* (up , dw , hor) and *polarity* ($+$, $-$). Each sensor saves in its local register R the first beacon that it receives for each orientation. The matching between the register positions and the orientations is also reported.

The static path Π_D is depicted as a dashed line in Fig. 6. Π_D is uniquely determined posing $F_x = d_{\min}/2$, $F_y = 0$, $F = (-F_x, -F_y)$, and $E = (x_E, y_E)$, where $x_E = Q_x + F_x$ and y_E can be either 0 or Q_y depending on the parity of the number of vertical scans. The *inter-waypoint distance* between two consecutive waypoints is denoted by I_w .

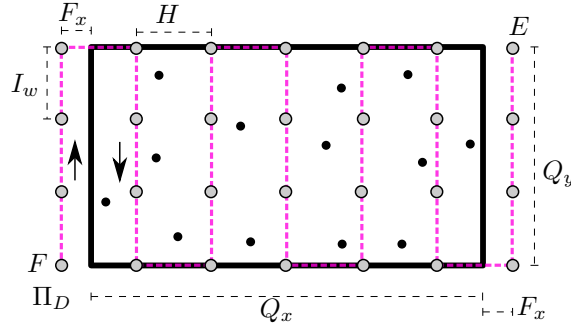


Figure 6: The static path Π_D of DIR (the segment \overline{EF} is not sketched)

From each vertical scan σ , the points of Q that we can precisely measure using any type of orientation are those at distance at least $d_{\min}/2$ and at most $(d_{\max} - 2I_w)/2$ from the scan σ . In fact, although the antennas of type *hor* can precisely measure the points at distance from d_{\min} up to d_{\max} from σ , the most stringent limits for the precise measurements come from the antennas of type *up* and *dw*. Therefore, any two consecutive vertical scans are fixed at distance no greater than at distance greater than $(d_{\max} - d_{\min} - 2I_w)/2$. Having fixed the first and the last scan respectively at $-F_x$ and $Q_x + F_x$, the length of H is fixed in order to evenly distribute $Q_x + 2F_x$ in stripes of width as tight as possible to the maximum value. In this way, the whole area is covered without wasting path length. Finally, observe that the left and right stripes of Q of width $d_{\min}/2$ adjacent to each vertical scan σ are not measured by σ to satisfy the d_{\min} constraint. The left and right stripes adjacent to σ are then measured by the scan that precedes σ and the scan that follows σ .

During the flight, for each waypoint, the drone sends the beacon's message along the six different orientations of beamwidth: up^+ , up^- , dw^+ , dw^- , hor^+ , and hor^- . When a sensor receives the drone's message from orientation ψ , for $\psi = d \cdot \pi/3$ and $d = 0, \dots, 5$, it first checks whether the d -th location of its register R is empty or not. In the first case, the sensor is receiving for the first time the beacon from the orientation d . In the second case, since the sensor has already heard that beacon from orientation d , the message is ignored. When the sensor receives one orientation for the first time, it replies to the drone with an ack message. The drone infers the distance from the time of the round-trip message, and sends to the sensor the measure. The sensor stores the measure in the local register R . The trilateration is performed by the sensor when it has received three measurements.

As explained previously, the localization error depends on the position of the three waypoints from which the point is ranged. From Eq. (6), the error is minimum when for each sensor $\beta_{\min} = \pi/3$. In our localization technique, the minimum angle at P is $\pi/3$ if and only if the sensor P resides at the intersection of the orientations of the three sectors centered at the waypoints $w_1(P)$, $w_2(P)$ and $w_3(P)$. Although it is not possible to achieve for every point P that the minimum angle is $\pi/3$, we can prove that the algorithm DIR provides [3]

$$\beta_{\min} \geq \frac{\pi}{3} - 2\theta \quad (7)$$

Considering Eq. (7), we are now in a position to rewrite Eq. (6) as a function that depends on h , d_{\min} and I_w . Inverting this expression we can ensure the precision required by the final user. In conclusion, according to [3], the localization precision can be expressed as:

$$\epsilon_L = \epsilon_s \cdot \sqrt{1 + \frac{h^2}{d_{\min}^2}} \cdot \frac{2\sqrt{1 + \left(\frac{I_w/2}{d_{\min}}\right)^2}}{1 - \sqrt{3}\left(\frac{I_w/2}{d_{\min}}\right)} \quad (8)$$

2.3 The OMNI algorithm

Now we present OMNI, which does not require specialized hardware such as directional antennas. Actually, OMNI is based on a standard omnidirectional antenna.

The omnidirectional antenna sends beacons with the drone's position isotropically. Since the sensors cannot distinguish from which direction they receive the beacon, it is difficult to select the waypoints that guarantee the desired geometry. For this reason, OMNI adopts a two phase approach. In the first phase, the sensors obtain a rough estimation of their position. In the second phase they use this estimation to pick among all the available waypoints the best ones, called *precise waypoints*, that equally divide the turn angle around the sensor itself to perform a trilateration and obtain a precise localization.

The static path Π_O is depicted in Fig. 7. The drone's mission starts at $F = (-F_x - H, -F_y)$, where $F_x = d_{\min}/2$, $F_y = \sqrt{3}(d_{\max} - I_w)/2$ and finishes at $E = (x_E, y_E)$, where $x_E = Q_x + F_x$ and y_E can be either 0 or Q_y . The inter-scan distance is set to $H = (d_{\max} - d_{\min} - 2I_w)/2$. Π_O consists of two vertical scans outside Q that are used to measure the sensors in the leftmost stripe of Q close to the vertical border, while the last vertical scan is at distance no larger than $\lfloor \frac{d_{\max} - 2I_w}{2} \rfloor$ from the rightmost border.

The behavior of the drone under OMNI is the same as during algorithm DIR. However, the behavior of the sensors is quite different. According to OMNI, until the first trilateration, the sensor stores all the measurements that it receives which are above the d_{\min} ground distance. As soon as the sensor has collected three distance measurements which belong to two different scans and are greater than the minimum ground distance, the sensor performs the first trilateration to compute a rough estimation of its position $\hat{P} = (x_{\hat{P}}, y_{\hat{P}})$.

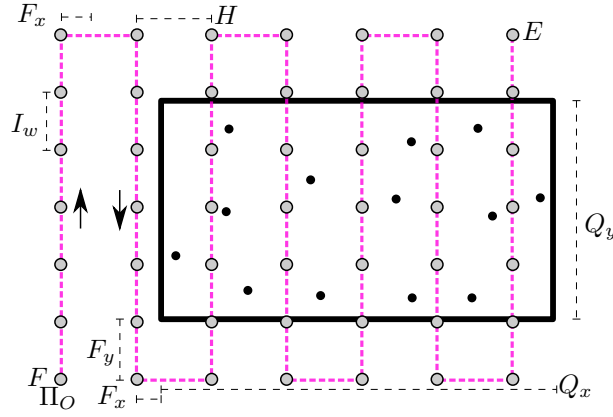


Figure 7: The static path Π_O of OMNI (the segment \overline{EF} is not sketched)

OMNI logically tessellates the area by diamonds (see Fig. 8). Then, from \hat{P} , the sensor locates the closest vertical scan σ on its left. Then, conceptually, the sensor derives the six rays that equally divide the turn angle around its current position. The intersections of such rays with the scan σ on the left of \hat{P} are then the most desirable positions as regard to the waypoint geometry (i.e., the β_{\min} constraint) from where taking the final measurements. However, such points may not coincide with waypoints because the drone takes measurements at regular distance and may also not satisfy the d_{\min} constraint. So, to find the three precise waypoints obeying all the constraints, the sensor locally computes the three precise waypoints $w_1(\hat{P}), w_2(\hat{P}), w_3(\hat{P})$ on the scans on its left. Selected $w_1(\hat{P}), w_2(\hat{P}), w_3(\hat{P})$, the sensor continues to hear to the drone until it has collected all the three precise waypoints and discards the measurements which are useless. Finally, the sensor computes the second precise trilateration using the precise waypoints, and the localization process is finished.

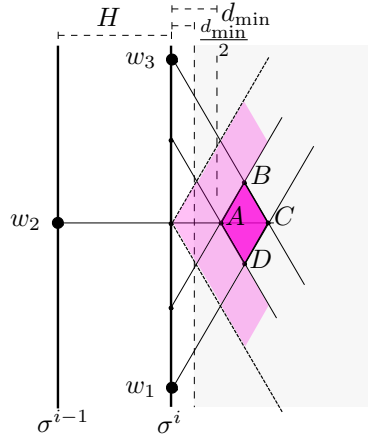


Figure 8: The tessellation

The localization error strictly depends on the position of the three precise waypoints w_1 and w_2 , and w_3 from which the point P is ranged. It has been proved in [2] that OMNI provides that

$$\beta_{\min} \gtrsim 2 \arctan \left(\frac{\frac{d_{\min}}{2}}{\sqrt{3} \frac{d_{\min}}{2} + 2I_w} \right) \quad (9)$$

Considering Eq. (9) and from Eq. (6) rewritten in terms of h , d_{\min} and I_w , the localization precision in OMNI can be expressed as [2]:

$$\epsilon_L = \epsilon_s \cdot \sqrt{1 + \frac{h^2}{d_{\min}^2}} \cdot \frac{\sqrt{1 + \left(\frac{\frac{d_{\min}}{2}}{\sqrt{3} \frac{d_{\min}}{2} + 2I_w} \right)^2}}{\left(\frac{\frac{d_{\min}}{2}}{\sqrt{3} \frac{d_{\min}}{2} + 2I_w} \right)} \quad (10)$$

3 Experimental Evaluation

We have implemented the SHORT, DIR, and OMNI localization algorithms in MATLAB programming language in order to compare their performance under a variety of different conditions.

Let first observe that OMNI and DIR belong to the class of the *precise* algorithms because they aim to guarantee the user-defined localization precision. Instead, SHORT belongs to the class of the *best-effort* algorithms that cannot ensure any a-priori guaranteed localization precision ϵ_L , but they return a very short static path. Consequently, we cannot use ϵ_L as the main metric to compare the performance of the three algorithms. Namely, SHORT does not respect d_{\min} and β_{\min} , and we cannot bound a-priori the localization error.

Considering the two different classes to which the three algorithms belong, in order to compare the goodness of them, we can only evaluate the *experimental position error*, expressed as the distance $\overline{PP'}$ between the original position P and the estimated position P' . For each drone's mission, we record the *worst experimental error* and then we compute the *error bound* $\overline{\epsilon_L}$ as the average value of the worst bound on the position error in all the missions. We also compute the 95%-confidence interval of the data reported in the experiments. Moreover, we will continue to evaluate the ability of DIR and OMNI of guaranteeing a-priori localization ϵ_L given in input to the algorithm. We compare and evaluate the three different algorithms under the metrics:

1. we evaluate the *path length*,
2. we compare *localization performance* in terms of *precision* and *error*, and
3. we analyze the difference of using *multilateration* instead of *trilateration*.

The goal of the experiment shown in Fig. 9, is to compare the length of the static paths Π_S , Π_D , and Π_O of the SHORT, DIR, and OMNI algorithms having fixed $I_w = 5$ m and $\epsilon_L = 0.30$ m for DIR and OMNI. DIR and OMNI have more or less the same number of vertical scans, but each vertical scan in OMNI goes well beyond the deployment area. Precisely, in OMNI, each vertical scan has length $2F_y + Q_y$, where $F_y = (d_{\max} - I_w)\sqrt{3}/2$, whereas $F_y = 0$ for DIR. Fig. 9 shows that Π_D is better than Π_O . The increase on the path length of the static path of OMNI is the paid price for not using specialized hardware. Note that the path length in OMNI is not monotonic decreasing because we use a fixed inter-scan value without resizing it as we do in DIR. Obviously, SHORT is the shortest static path regardless of the length of the communication radius r , but one has to remember that SHORT requires to solve off-line an instance of TSP before the drone can start its mission. DIR is twice as long as SHORT. SHORT is the shortest path but it does not have neither d_{\min} nor β_{\min} constraints, and thus its precision is not guaranteed (see Fig. 10 for the analysis of the precision of SHORT).

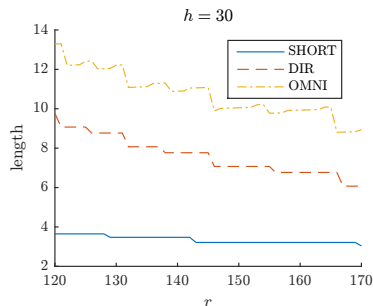


Figure 9: Path length in SHORT, DIR, and OMNI algorithms

Note that d_{\max} , and thus the communication range r , is the parameter that mostly influences the length of the path in DIR and OMNI. For this reason, we omitted to report the value of d_{\min} adopted in Fig. 9 for DIR and OMNI.

In the following, we compare in Fig. 10 the localization performance in terms of user-defined precision and error.

In the first experiment shown in Fig. 10(a) we compare the user-defined precision ϵ_L for the precise algorithms DIR and OMNI. Specifically, we want to experimentally verify that our bound holds, and thus $\overline{\epsilon_L} < \epsilon_L$. In DIR and OMNI we set $I_w = \{5, 10\}$ m and $\epsilon_L = 0.30$ m. Given the localization precision ϵ_L , we select d_{\min} for DIR and OMNI by applying Eq. (8) and Eq. (10), respectively, and compare it with the results from the experiments. It is worthy to note that the error bound in Fig. 10(a) is always smaller than the user-defined localization precision $\epsilon_L = 0.30$ m. The OMNI algorithm is slightly more precise than DIR because OMNI uses values of d_{\min} larger than DIR, and the β_{\min} angle is larger in OMNI than DIR. Moreover, OMNI uses two trilaterations.

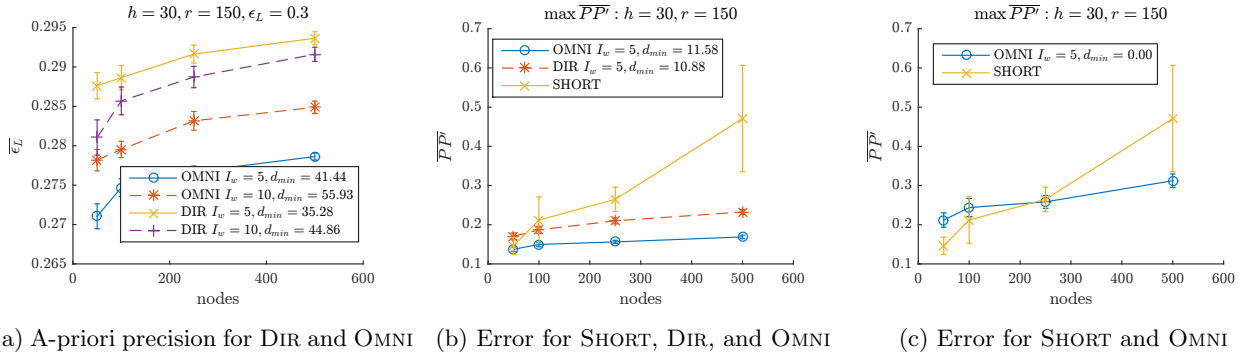


Figure 10: Comparing the localization performances

In the second experiment, reported in Fig. 10(b), we compare the localization error among all the three algorithms, considering also the path length. DIR and OMNI run using the values of d_{\min} and I_w that guarantee a maximum error of $\epsilon_L = 1$ m. For SHORT, instead, we just use for each sensor the three waypoints that form the vertices of the triangle that better circumscribes the sensor itself. Although in SHORT the three waypoints surround the point to be localized, neither minimal ground distance d_{\min} nor minimum angle β_{\min} constraints are respected in a predefined way. Thus, the error for SHORT increases in Fig. 10(b). In fact, even if the sensor is inside the triangle formed by the three waypoints, it is sufficient that it is close to one of the vertices to break the d_{\min} constraint. Hence, it is easy to see from Eq. (8) that, when the ground distance tends to 0, the error blows up. Moreover, the reported error and the confidence interval of SHORT is higher when n is large than when n is small because the probability of encountering sensors in the worst position increases. Contrary, DIR and OMNI have a good level of precision since all the four constraints d_{\max} , d_{\min} , β_{\min} , and *non-linearity*, are satisfied and as a consequence of the setting of the parameters I_w and d_{\min} , they guarantee an a-priori localization error of $\epsilon_L = 1$ m. It is important to note that the path length of SHORT is 3.2 km, which is less than half the path length of DIR (6 km) and OMNI (8.2 km).

In the third experiment depicted in Fig. 10(c), we have relaxed the d_{\min} constraint accepting any measurement, i.e., $d_{\min} = 0$. With this experiment we want to evaluate if, paying a higher localization error, we can considerably shorten the path of the precise algorithms. First, note that the d_{\min} constraints cannot be relaxed for DIR, since $\theta = \arctan \frac{I_w/2}{d_{\min}}$. Hence, in DIR, d_{\min} must be positive. In omni we can set $d_{\min} = 0$. The error increases, but it remains smaller than that of SHORT. Nonetheless, the path length of OMNI is still the double of that of SHORT. In conclusion, OMNI and DIR have been mainly designed to be precise, and reducing the precision does not reduce the path length. So, precision cannot be traded for path length in OMNI and DIR.

Finally, we compare our algorithms when multilateration is used instead of trilateration. A crucial finding of our experiments is that multilateration helps when the algorithm is best-effort, but it does not help when the algorithms are precise.

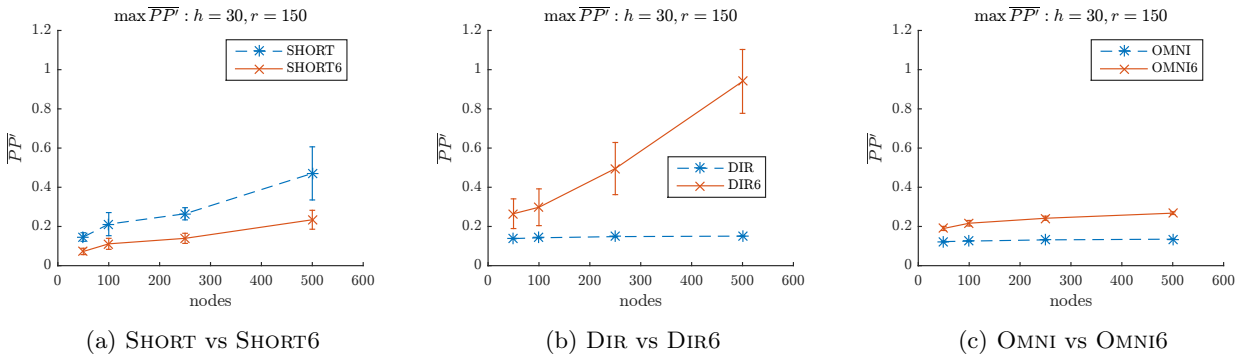


Figure 11: Multilateration vs Trilateration (1)

In the experiment shown in Fig. 11 we want to analyze whether an optimal geometry of three waypoints is better than six generic waypoints, or not. Specifically, SHORT6, DIR6, and OMNI6 are, respectively, the modified version of SHORT, DIR, and OMNI, which localize each sensor exploiting the first (in order of time) six non-collinear waypoints that a sensor hears from the drone. Fig. 11(b) and Fig. 11(c) show that a good geometry, is

better than a blind multilateration. It is not sufficient to increase the number of waypoints for obtaining a smaller error. Namely, since DIR6 and OMNI6 choose the first three waypoints from a vertical scan and the other three from the subsequent one, β_{\min} can be very small. Although OMNI6 (see Fig. 11(c)) is less precise than OMNI, the localization degrades less than between DIR and DIR6 (see Fig. 11(b)). We believe that this is due to the fact that in general OMNI and OMNI6, according to the regular omnidirectional antenna, can take measurements at distances greater than compared to those taken in DIR6 with directional antennas. On the other hand, Fig. 11(a) highlights that using the first six waypoints for SHORT6 the precision improves. Although no geometry has been set in SHORT6, the experimental error is smaller than that in the original algorithm SHORT which aims to build a weak geometry formed by isosceles triangles. SHORT performs as the common belief: more waypoints help for improving the localization. Therefore, multilateration helps precision for the best-effort algorithm SHORT.

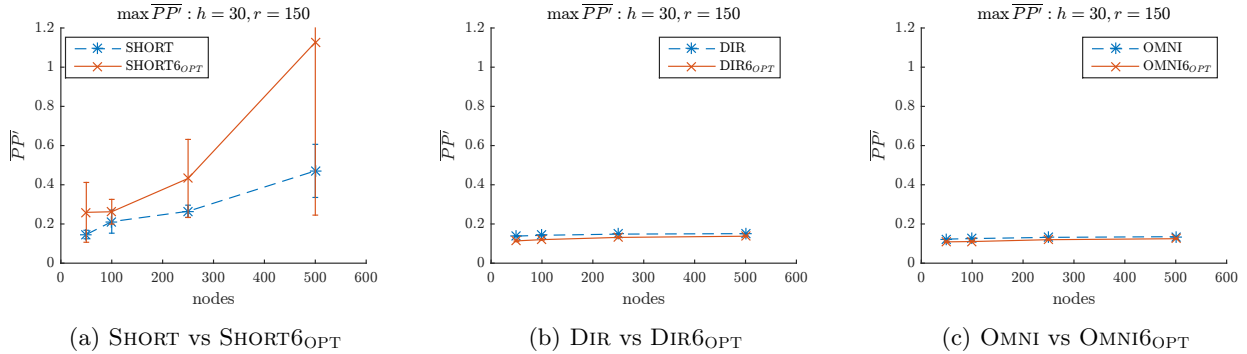


Figure 12: Multilateration vs Trilateration (2)

In the experiment shown in Fig. 12 we study whether multilateration improves the localization when the geometry constraints are respected also by the six measurements. Specifically, be $\text{SHORT6}_{\text{OPT}}$ the modified version of SHORT which considers the initial three associated vertices of the triangle that better circumscribes the sensor plus the three midpoints along each triangle’s side. DIR6_{OPT} is the modified version of DIR which localizes all the sensors exploiting all the different possible six orientations that a sensor can hear. Moreover, $\text{OMNI6}_{\text{OPT}}$ is the modified version of OMNI which uses for each sensor the optimal triple of waypoints plus another triple, clone of the first one. Fig. 12(b) and Fig. 12(c) show that the geometry of the waypoints, for any algorithm belonging to the precise class, is essential to localize the sensors with a small error. In practice for DIR and OMNI, a non-blind multilateration works almost the same than as the simple trilateration. However, since the precision is almost the same for trilateration and multilateration when both satisfy the geometry constraints, there is no reason to pay an extra computational cost. Even in this experiment, in Fig. 12(a), SHORT behaves differently from DIR and OMNI: with $\text{SHORT6}_{\text{OPT}}$ the precision deteriorates. This shows that it is difficult to define which is a good geometry for an algorithm without rigid constraints for precision.

In summary we believe that it is difficult to achieve small localization error without a careful design of the localization algorithms. On the other hand, when we have a well defined geometry that guarantees precision, trilateration is good enough.

4 Conclusion and Future Work

In this paper, we surveyed three localization algorithms that replace multiple fixed anchor sensors with a flying drone. We investigated the impact of multilateration for the three different algorithms. For DIR and OMNI, which are precise algorithms that measure the sensors obeying to a rigid geometry, a multilateration that just increases the number of waypoints is not useful to improve the precision of the localization. A multilateration that increases the number of waypoints respecting the geometry improves localization in a negligible way. So we can conclude that when the waypoints for each sensor follow a well pondered geometry, multilateration is not useful. Whereas, the precision of the SHORT algorithm, which follows a best-effort policy in selecting the waypoints for each sensor, benefits of taking more measurements. For the best-effort algorithms, the design of sophisticated multilateration techniques that preserve geometry requires further investigation.

In our future works, in addition to further look for short drone’s paths that preserve precision, we intend to analyze the energy consumption of the localization algorithms on both the drone and the sensors side, considering also the number of the waypoints. We also wish to perform a test-bed with a drone of our localization algorithms.

Acknowledgments

The work has been partially supported by GEO-SAFE (H2020-691161), “RISE” Fondazione CR-PG (code 2016.0104.021), “Project Static Path Planning for Drones to Secure Localization” granted by Fondo Ricerca di Base 2015 University of Perugia, and “GNCS-INdAM”.

References

- [1] A. Papadopoulos, A. Navarra, J. A. McCann, and C. M. Pinotti, “VIBE: An energy efficient routing protocol for dense and mobile sensor networks,” *Journal of Network and Computer Applications*, vol. 35, no. 4, pp. 1177–1190, 2012.
- [2] C. M. Pinotti, F. Betti Sorbelli, P. Perazzo, and G. Dini, “Localization with guaranteed bound on the position error using a drone,” in *Proceedings of the 14th ACM International Symposium on Mobility Management and Wireless Access, MobiWac '16*, (New York, NY, USA), pp. 147–154, ACM, 2016.
- [3] F. B. Sorbelli, S. K. Das, C. M. Pinotti, and S. Silvestri, “Precise localization in sparse sensor networks using a drone with directional antennas,” in *Proceedings of the 19th International Conference on Distributed Computing and Networking, ICDCN '18*, (New York, NY, USA), pp. 34:1–34:10, ACM, 2018.
- [4] L. Gupta, R. Jain, and G. Vaszkun, “Survey of important issues in uav communication networks,” *IEEE Communications Surveys Tutorials*, vol. 18, pp. 1123–1152, Secondquarter 2016.
- [5] C. Yuan, Y. Zhang, and Z. Liu, “A survey on technologies for automatic forest fire monitoring, detection, and fighting using unmanned aerial vehicles and remote sensing techniques,” *Canadian Journal of Forest Research*, vol. 45, no. 7, pp. 783–792, 2015.
- [6] P. Perazzo, F. B. Sorbelli, M. Conti, G. Dini, and C. M. Pinotti, “Drone path planning for secure positioning and secure position verification,” *IEEE Transactions on Mobile Computing*, vol. 16, pp. 2478–2493, Sept 2017.
- [7] Enac, *UAV regulations in Italy*, 2018 (accessed April 10, 2018). <https://goo.gl/vgktKd>.
- [8] G. Heredia, F. Caballero, I. Maza, L. Merino, A. Viguria, and A. Ollero, “Multi-unmanned aerial vehicle (uav) cooperative fault detection employing differential global positioning (dgps), inertial and vision sensors,” *Sensors*, vol. 9, no. 9, pp. 7566–7579, 2009.
- [9] DecaWave, *DecaWave Ltd: ScenSor SWM1000 Module*, 2018 (accessed April 10, 2018). <http://www.decawave.com/products/dwm1000-module>.
- [10] F. B. Sorbelli, S. K. Das, C. M. Pinotti, and S. Silvestri, “On the accuracy of localizing terrestrial objects using drones,” in *IEEE International Conference on Communications, ICC 2018*, 2018.
- [11] D. Koutsonikolas, S. M. Das, and Y. C. Hu, “Path planning of mobile landmarks for localization in wireless sensor networks,” *Comput. Commun.*, vol. 30, pp. 2577–2592, Sept. 2007.
- [12] R. Huang and G. V. Zaruba, “Static path planning for mobile beacons to localize sensor networks,” in *Pervasive Computing and Communications Workshops, 2007. PerCom Workshops' 07. Fifth Annual IEEE International Conference on*, pp. 323–330, IEEE, 2007.
- [13] J. Jiang, G. Han, H. Xu, L. Shu, and M. Guizani, “LMAT: Localization with a mobile anchor node based on trilateration in wireless sensor networks,” in *2011 IEEE Global Telecommunications Conference - GLOBE-COM 2011*, pp. 1–6, Dec 2011.
- [14] H. T. Hu, F. C. Chen, and Q. X. Chu, “A compact directional slot antenna and its application in MIMO array,” *IEEE Transactions on Antennas and Propagation*, vol. 64, pp. 5513–5517, Dec 2016.